Technical Note

Title:

Modelling the stance leg in 2D analyses of sprinting: inclusion of the MTP joint affects joint kinetics (corrected version)

Authors:

Neil E. Bezodis[a,b], Aki I.T. Salo[b], Grant Trewartha[b]

bezodisn@smuc.ac.uk.

A.Salo@bath.ac.uk

G.Trewartha@bath.ac.uk

Affiliations:

[a]School of Sport, Health and Applied Science, St Mary's University College, Twickenham, UK.

[b]Sport, Health and Exercise Science, University of Bath, UK.

Keywords:

Biomechanics, foot model, joint moments, metatarsal-phalangeal, sprint start

Abstract

Two-dimensional analyses of sprint kinetics are commonly undertaken but often ignore the metatarsal-phalangeal (MTP) joint and model the foot as a single segment. The aim of this study was to quantify the role of the MTP joint in the early acceleration phase of a sprint and to investigate the effect of ignoring the MTP joint on the calculated joint kinetics at the other stance leg joints. High-speed video and force platform data were collected from four to five trials for each of three international athletes. Resultant joint moments, powers and net work at the stance leg joints during the first stance phase after block clearance were calculated using three different foot models. Considerable MTP joint range of motion (>30°) and a peak net MTP plantar flexor moment of magnitude similar to the knee joint were observed, thus highlighting the need to include this joint for a more complete picture of the lower limb energetics during early acceleration. Inclusion of the MTP joint had minimal effect on the calculated joint moments, but some of the calculated joint power and work values were significantly ($P < 0.05$) and meaningfully affected, particularly at the ankle. The choice of foot model is therefore an important consideration when investigating specific aspects of sprinting technique.

Introduction

Biomechanists often develop linked-segment rigid body models comprising the segments and joints deemed to be of sufficient importance to an activity of interest. When joint kinetics are also required, these models are typically incorporated within inverse dynamics analyses (IDA). The lower limb joint moments in sprinting have been widely investigated using IDA to understand the two-dimensional (2D) sagittal plane movements occurring in the primary plane (e.g. Mann, 1981; Jacobs & van Ingen Schenau, 1992; Johnson & Buckley, 2001; Kuitunen et al., 2002; Hunter et al., 2004; Mero et al., 2006; Bezodis et al., 2008). These studies all used a three segment representation of the leg which included thigh, shank and foot segments. Whilst the thigh and shank segments were consistently modelled from hip to knee, and knee to ankle joint centres, respectively, some of these studies modelled the foot from the ankle to the distal hallux, and others to the metatarsal-phalangeal (MTP) joint. Kinematic 2D analyses of sprinting have revealed that rotation in excess of 20° occurs about the MTP joint (Stefanyshyn & Nigg, 1997; Krell & Stefanyshyn, 2006; Toon et al., 2009); by ignoring this motion any resultant joint moments generated about the MTP joint, and their consequent effects, are also ignored.

Since Elftman (1940) proposed that the resultant moments about the MTP joint are large enough to warrant consideration in sprint analyses, it appears that only Stefanyshyn & Nigg (1997) have included an MTP joint when calculating 2D joint kinetics during sprinting. Stefanyshyn & Nigg (1997) observed peak resultant MTP plantarflexor moments of up to 120 N·m (at the 15 m mark), and up to 70 J of energy was found to be absorbed at the MTP joint, accounting for around 32% of the total energy absorbed in the four leg joints (MTP, ankle, knee, hip) during ground contact. These results suggest that it could be important to include the MTP joint when conducting a sprint-related IDA, but the extent to which this would affect the calculated kinetics at the other joints in the leg model is not clear. Whilst using different distal endpoints for a single foot segment could slightly affect the magnitude of the calculated resultant joint moments in the stance leg, it is proposed that ignoring the MTP joint will have a more pronounced effect. The aim of this study was thus to investigate the effect of three different foot models on leg joint kinetics during a stance phase in sprinting.

Methods

A single-subject approach was adopted since the foot models may affect the joint kinetics on an individual basis. However, to widen the potential application of the findings, this within-subject analysis was repeated across three relatively heterogeneous trained athletes (Table 1). Following ethical approval and written informed consent, a high-speed digital video camera (Motion Pro®, HS-1, Redlake, USA; 200 Hz) was used to capture full body sagittal plane kinematic data during the first stance phase of maximal effort sprints to 30 m on an indoor track as a part of larger research study. The camera was positioned 25.00 m away from the centre of the running lane, perpendicular to the direction of the sprint, 0.95 m in front of the start line and with the lens centre 1.00 m above the ground. An area of 2.000 m horizontally × 1.600 m vertically was calibrated, and the camera collected images at a resolution of 1280 × 1024 pixels with a 1/1000 s shutter speed. A start line was positioned on the track such that the first foot contact would occur near the centre of a 0.900 × 0.600 m covered force platform (Kistler, 9287BA, Kistler Instruments Ltd., Switzerland; 1000 Hz) embedded in the track. Each trial was initiated by a trigger button which activated a sounder (to which the athletes reacted), the force platform, and a series of 20 LEDs (Wee Beasty Electronics, UK) to allow synchronisation of the video and ground reaction force (GRF) data to the nearest 1 ms.

****Table 1 near here****

From the video files, six points (shoulder, stance hip, knee, ankle and mid MTP joint centres, and distal hallux) were manually digitised and affine scaled from 10 frames prior to touchdown until 10 frames after toe-off (Peak Motus®, v. 8.5, Vicon, USA). It has previously been proposed that displacement and force data used for IDA should be subjected to the same level of smoothing to prevent artificial impact joint moments being introduced (van den Bogert & de Koning, 1996; Bisseling & Hof, 2006). The displacement and GRF data were therefore passed through a fourth-order Butterworth filter using the mean optimal cut-off frequency (24 Hz) determined from a residual analysis of all displacement data (Winter, 1990).

To create the experimental conditions, the stance leg was represented using three different models (Figure 1). The thigh and shank segments were consistently modelled from hip to knee, and knee to ankle joint centres, respectively. For two of the models, the foot was modelled as a single segment, firstly from ankle to distal hallux (model 3segH) and secondly from ankle to MTP (3segM). The final model (4seg) included a two segment foot, comprising a rearfoot segment from ankle to MTP and a forefoot segment from MTP to distal hallux. Individual-specific segmental inertia data were obtained using the model of Yeadon (1990), which provided appropriate data for the foot in all three models. To account for the spiked shoes, 0.20 kg was added to the mass of the foot (e.g. Hunter et al., 2004). For model 4seg, this was divided between the segments based on the ratio of forefoot:rearfoot length. Joint angles were determined, and were subjected to second central difference calculations (Miller & Nelson, 1973) to derive corresponding velocity and acceleration time-histories.

****Figure 1 near here****

Prior to filtering, the raw GRF data were downsampled to 200 Hz, and centre of pressure data were calculated accounting for the thickness of the track surface. These downsampled GRF data were combined with the kinematic and inertia data in an IDA (Elftman, 1939; Winter, 1990). Since contact only occurred with the forefoot segment during this early part of a sprint for these three sprinters, all calculations started with the GRF being applied at the centre of pressure to the most distal segment and proceeded in a distal-to-proximal fashion (i.e. there was no need to share the GRF between the forefoot and rearfoot in model 4seg). Contact with only the forefoot was confirmed as a normal occurrence during the first stance phase of a sprint through an additional qualitative analysis of the 13 University-level sprinters studied by Bezodis et al. (2010). Joint power was calculated as the product of resultant moment and angular velocity, and net joint work was calculated as the time-integral of power. For all calculated variables, extension/plantarflexion was defined as positive. Mean and standard deviations were calculated for all variables for each athlete. Repeated measures ANOVA comparisons (SPSS 15.0 for Windows, SPSS Inc., USA) were run for dependent variables (peak resultant extensor joint moments and powers, and net joint work) for all three athletes separately. When a significant ($P < 0.05$) main effect was observed, Bonferroni *post hoc* tests were calculated to investigate the pairwise differences.

Results

The mean horizontal velocity of the athletes at touchdown was 3.29 ± 0.22 m/s, and during the first stance phase (mean duration = 0.188 ± 0.009 s), velocity increased by 1.27 ± 0.11 m/s. The MTP angle ranges of motion during stance for athletes A, B, and C were 34 ± 7°, 30 ± 7°, and 31 ± 1°, respectively. Time histories for MTP joint angle, angular velocity, resultant moment, and power from model 4seg are presented in Figure 2. To illustrate the general temporal patterns of the joint kinetic data during stance when using each of the three leg models, Figure 3 presents the mean resultant moment and power time histories for the ankle, knee, and hip joints for athlete C. Differences between leg models were essentially non-existent when considering joint moment patterns at the ankle, knee and hip joints (some significant differences were observed due purely to the systematic nature of these small effects; Table 2). However, some significant and more meaningful differences were observed in joint power and work values due to variations in the calculated angular velocity data between leg models, particularly at the ankle joint.

****Figures 2a-d near here****

****Table 2 near here****

****Figures 3a-f near here****

Discussion

The MTP joint rotated through mean ranges of motion in excess of 30° for each of the three athletes (Figure 2a), similar to previous results (Krell & Stefanyshyn, 2006; Toon et al., 2009). The mean peak MTP resultant joint moments ranged from 67 to 143 N·m (1.1–1.7 N·m/kg; Figure 2c), and are due to both the biological structures crossing the MTP joint and to the spiked shoe (Oleson et al., 2005). Due to these moments and the observed angular velocities (Figure 2b), the MTP joint is clearly important in absorbing energy during the stance phase (Figure 2d), reaching magnitudes of up to 50 J for some trials of athlete C (Table 2). For athletes A and B in particular, the magnitudes of the resultant joint moments, power and net work at the MTP joint were comparable to those of the knee joint, and it therefore appears important to include this joint in analyses of the energetics of sprinting to obtain a more complete understanding of the internal kinetics. Although there were systematic and statistically significant differences in ankle and hip joint moment (Table 2), these were very small in magnitude (typically less than 1 Nm at the ankle joint). When placed in the context of the typical within-athlete variation based on the standard deviation data presented in Table 2, the practical significance of these differences due to the choice of leg model is clearly minimal, opposing the suggestion in our original paper (Bezodis et al., 2012). The observed significant differences in ankle joint work and power (Table 2 and Figure 3b) between the models which linked the ankle to the MTP joint (3segM and 4seg) and the model which linked the ankle to the distal hallux

(3segH) are more practically meaningful. These differences can be attributed to contrasting ankle joint angular velocities between these two three-segment leg models, and they highlight that the choice of distal endpoint for a single segment foot could influence the results if absolute values of ankle joint power or work are of interest.

The foot is clearly multisegmental and three dimensional, and while inclusion of the MTP joint reveals ‘within-foot’ energetics that would be overlooked if using a single-segment representation, it is acknowledged that it remains a simplification. However, coaches and biomechanists are often interested in the 2D mechanics of sprinting (e.g., Mann, 1981; Jacobs & van Ingen Schenau, 1992; Johnson & Buckley, 2001; Kuitunen et al., 2002; Hunter et al., 2004; Mero et al., 2006; Bezodis et al., 2008) due to the largely planar nature of the skill in addition to time and equipment/instrumentation constraints.

The results of the current study revealed that the resultant joint moments, power and net work at the MTP joint are large enough to warrant consideration in future kinetic analyses of early acceleration. Due to the increased requirement for energy absorption combined with the considerable motion previously observed at the MTP joint during maximum velocity sprinting (Krell and Stefanyshyn, 2006), it is likely that the MTP joint should be considered in kinetic analyses throughout all phases of a sprint. However, if the specific kinetics of just the ankle, knee and/or hip joint are the sole focus of a study, a three segment leg model will yield appropriate data providing that the MTP joint is used as the distal endpoint for the foot segment if ankle joint power or work data are of interest.

Acknowledgements

The authors are grateful to the University of Wales Institute, Cardiff and the National Indoor Athletics Centre for providing facilities for data collection. Dr Ian Bezodis is thanked for his assistance in relation to the data collection.

References

Bezodis, I. N., Kerwin, D. G., & Salo, A. I. T. (2008). Lower-limb mechanics during the support phase of maximum-velocity sprint running. *Medicine and Science in Sports and Exercise, 40,* 707-715.

Bezodis, N. E., Salo, A. I. T., & Trewartha, G. (2010). Choice of sprint start performance measure affects the performance-based ranking within a group of sprinters: which is the most appropriate measure? *Sports Biomechanics, 9,* 258-269.

Bisseling, R. W., & Hof, A. L. (2006). Handling of impact forces in inverse dynamics. *Journal of Biomechanics, 39,* 2438-2444.

van den Bogert, A. J., & de Koning, J. J. (1996). On optimal filtering for inverse dynamics analysis. In J. A. Hoffer, A. Chapman, J. J. Eng, A. Hodgson, T. E. Milner & D. Sanderson (Eds.), *Proceedings of the IXth Biennial Conference of the Canadian Society for Biomechanics* (pp. 214-215). Vancouver: University Press.

Elftman, H. (1939). Forces and energy changes in the leg during walking. *American Journal of Physiology, 125*, 339-356.

Elftman, H. (1940). The work done by muscles in running. *American Journal of Physiology, 129,* 672-684.

Hunter, J. P., Marshall, R. N., & McNair, P. J. (2004). Segment-interaction analysis of the stance limb in sprint running. *Journal of Biomechanics, 37,* 1439-1446.

Jacobs, R., & van Ingen Schenau, G. J. (1992). Intermuscular coordination in a sprint push-off. *Journal of Biomechanics, 25,* 953-965.

Johnson, M. D., & Buckley, J. G. (2001). Muscle power patterns in the mid-acceleration phase of sprinting. *Journal of Sports Sciences, 19,* 263-272.

Krell, J. B., & Stefanyshyn, D. J. (2006). The relationship between extension of the metatarsophalangeal joint and sprint time for 100 m Olympic athletes. *Journal of Sports Sciences, 24,* 175-180.

Kuitunen, S., Komi, P. V., & Kyröläinen, H. (2002). Knee and ankle joint stiffness in sprint running. *Medicine and Science in Sports and Exercise, 34,* 166-173.

Mann, R. V. (1981). A kinetic analysis of sprinting. *Medicine and Science in Sports and Exercise, 13,* 325-328.

Mero, A., Kuitunen, S., Harland, M., Kyröläinen, H., & Komi, P. V. (2006). Effects of muscle-tendon length on joint moments and power during sprint starts. *Journal of Sports Sciences, 24,* 165-173.

Miller, D., & Nelson, R. (1973). *Biomechanics of sport: a research approach*. Philadelphia, PA: Lea & Febiger.

Oleson, M., Adler, D., & Goldsmith, P. (2005). A comparison of forefoot stiffness in running and running shoe bending stiffness. *Journal of Biomechanics, 38,* 1886-1894.

Stefanyshyn, D. J., & Nigg, B. M. (1997). Mechanical energy contribution of the metatarsophalangeal joint to running and sprinting. *Journal of Biomechanics, 30,* 1081-1085.

Stefanyshyn, D. J., & Nigg, B. M. (2000). Influence of midsole bending stiffness on joint energy and jump height performance. *Medicine and Science in Sports and Exercise, 32,* 471-476.

Toon, D., Williams, B., Hopkinson, N., & Caine, M. (2009). A comparison of barefoot and sprint spike conditions in sprinting. *Journal of Sports Engineering and Technology, 223,* 77-87.

Winter, D. A. (1990). *Biomechanics and motor control of human movement*. New York: Wiley.

Yeadon, M. R. (1990). The simulation of aerial movement-II: a mathematical inertia model of the human-body. *Journal of Biomechanics, 23,* 67-74.

Table 1. Descriptive characteristics for the three athletes.

	A	B	C
Age [years]	26	21	20
Gender	Female	Male	Male
Mass [kg]	60.5	82.6	86.9
Height [m]	1.76	1.81	1.78
PB [s]	12.72[#]	10.14*	10.28*
No. of trials	4	5	5

[#] indicates personal best (PB) for 100 m hurdles; * indicates PB for 100 m; A: World Indoor Championships medalist; B: European Indoor Championships medalist; C: European Indoor Championships finalist

Table 2. Peak resultant joint moments and powers, and net work, for each of the three athletes using each of the three leg models (mean ± *s*).

	Athlete	3segH	3segM	4seg
Peak resultant MTP joint extensor moment [N·m]	A			67 ± 6
	B			107 ± 5
	C			143 ± 8
Peak resultant ankle joint extensor moment [N·m]	A*	210 ± 9[b,c]	210 ± 9[a,c]	210 ± 9[a,b]
	B*	351 ± 19[b,c]	351 ± 19[a,c]	351 ± 19[a,b]
	C*	363 ± 6[b,c]	364 ± 6[a,c]	364 ± 6[a,b]
Peak resultant knee joint extensor moment [N·m]	A	75 ± 14	75 ± 14	75 ± 14
	B	67 ± 21	66 ± 22	66 ± 22
	C	172 ± 18	172 ± 18	172 ± 19
Peak resultant hip joint extensor moment [N·m]	A	137 ± 14	136 ± 14	136 ± 14
	B*	237 ± 56[c]	245 ± 53	247 ± 53[a]
	C*	264 ± 33	266 ± 32	262 ± 31
Peak positive MTP joint power [W]	A			253 ± 106
	B			612 ± 418
	C			219 ± 109
Peak positive ankle joint power [W]	A	2177 ± 326	2228 ± 260	2221 ± 259
	B*	2629 ± 236[b,c]	2970 ± 189[a,c]	2963 ± 188[a,b]
	C*	3378 ± 83[b,c]	3891 ± 79[a,c]	3881 ± 79[a,b]
Peak positive knee joint power [W]	A	423 ± 28	420 ± 33	425 ± 37
	B	383 ± 200	350 ± 191	351 ± 191
	C*	1053 ± 95[c]	1051 ± 96[c]	1062 ± 97[a,b]
Peak positive hip joint power [W]	A	1292 ± 208	1295 ± 213	1268 ± 211
	B*	2980 ± 696[c]	3088 ± 651	3107 ± 647[a]
	C*	2853 ± 479	2868 ± 472[c]	2815 ± 469[b]
Net MTP joint work [J]	A			-22 ± 5
	B			-26 ± 10
	C			-46 ± 4
Net ankle joint work [J]	A*	49 ± 9[b,c]	68 ± 6[a,c]	68 ± 6[a,b]
	B*	81 ± 13[c]	97 ± 16[c]	96 ± 16[a,b]
	C*	91 ± 7[b,c]	127 ± 9[a,c]	126 ± 9[a,b]
Net knee joint work [J]	A*	20 ± 13[b,c]	19 ± 12[a]	18 ± 12[a]
	B*	-5 ± 18[b,c]	-9 ± 17[a]	-9 ± 17[a]
	C*	82 ± 17[b,c]	80 ± 17[a]	80 ± 17[a]
Net hip joint work [J]	A*	76 ± 15[b,c]	78 ± 15[a,c]	80 ± 15[a,b]
	B*	108 ± 20[b,c]	111 ± 19[a,c]	114 ± 19[a,b]
	C*	111 ± 22[b,c]	113 ± 22[a,c]	115 ± 21[a,b]

* significant effect of leg model ($P < 0.05$); [a] significantly different from 3segH; [b] significantly different from 3segM; [c] significantly different from 4seg.

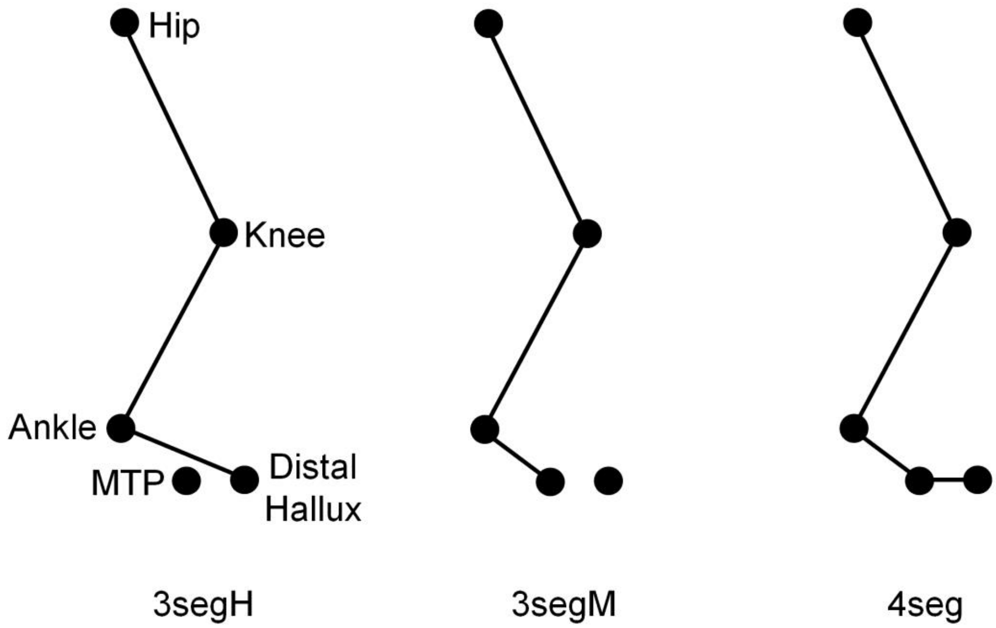

Figure 1. The three models used to represent the stance leg.

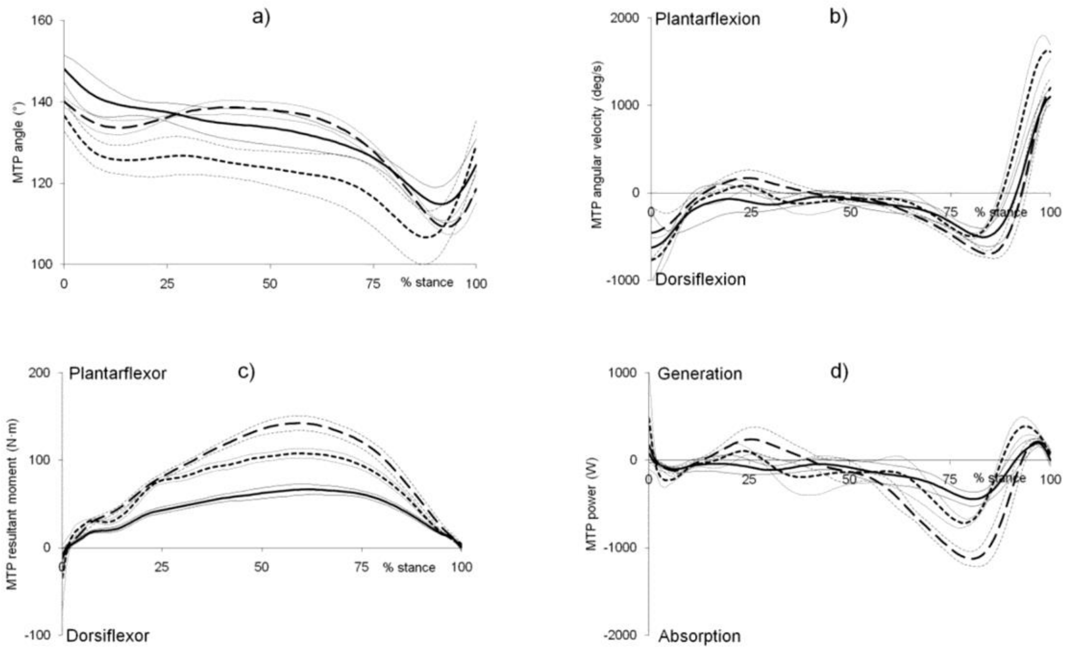

Figures 2a-d. Time-histories (mean ± *s*) for joint angle (a), angular velocity (b), resultant moment (c) and power (d) at the MTP joint during stance for each of the three athletes calculated using the 4seg model (athlete A = solid line, athlete B = dotted line, athlete C = dashed line). MTP joint angle was calculated as the angle between the rearfoot and forefoot segments on the proximal side of the foot.

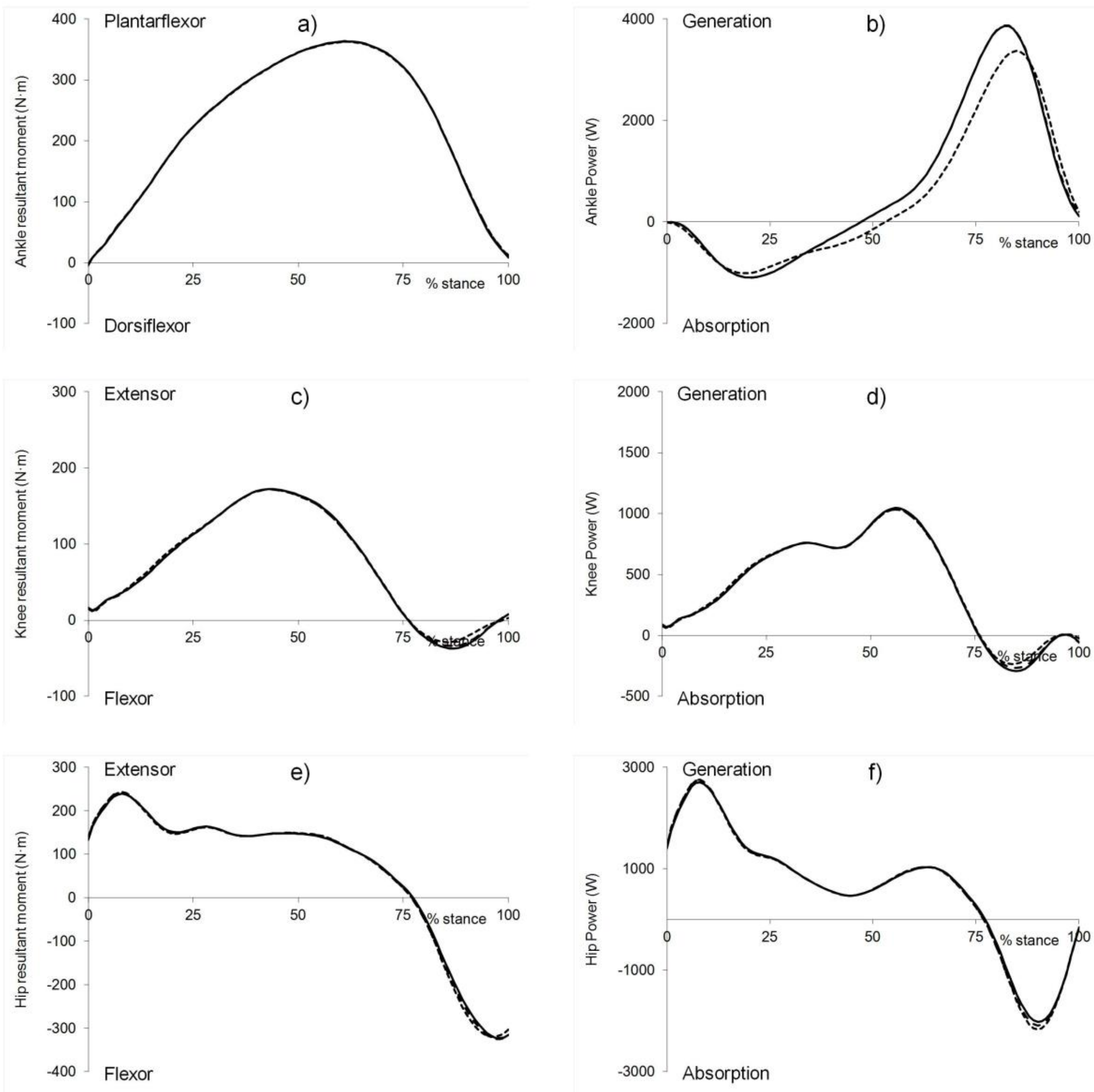

Figure 3. Mean time histories for ankle resultant joint moment (a) and power (b), knee resultant joint moment (c) and power (d), hip resultant joint moment (e) and power (f) for athlete C (model 4seg = solid line, 3segH = dotted line, 3 segM = dashed line).